



# Quantum-enhanced optomechanical accelerometer

WEI LI,<sup>1,2,†</sup> QINGHUI LI,<sup>1,†</sup> YUFAN WANG,<sup>1</sup> YAJUN WANG,<sup>1,2</sup> LONG TIAN,<sup>1,2</sup> SHAOPIING SHI,<sup>1,2</sup> AND YAOHUI ZHENG<sup>1,2,\*</sup>

<sup>1</sup>State Key Laboratory of Quantum Optics Technologies and Devices, Institute of Opto-Electronics, Shanxi University, Taiyuan 030006, China

<sup>2</sup>Collaborative Innovation Center of Extreme Optics, Shanxi University, Taiyuan 030006, China

<sup>†</sup>These authors contributed equally to this work.

\*Corresponding author: yzheng@sxu.edu.cn

Received 11 July 2025; revised 19 September 2025; accepted 29 September 2025; posted 1 October 2025 (Doc. ID 573361); published 31 October 2025

Acceleration sensing, an essential branch of quantum sensing, faces a fundamental trade-off between resolution and bandwidth. Here, we present a quantum-enhanced optomechanical accelerometer (QEOMA), simultaneously achieving the improvement of the sensing resolution and bandwidth in contrast with a classical counterpart. By tailoring quantum squeezed light, the optomechanical cooperativity is significantly raised, extending the sensing bandwidth. Quantum squeezed light increases the equivalent  $Q$  value of the optomechanical accelerometer owing to the reduction of the mechanical damping rate, driving the resolution improvement at the resonance frequency. At off-resonance frequencies, the resolution improvement is attributed to the imprecision noise reduction. We obtain the measured noise power spectrum and inferred acceleration resolution for the (3,3), (4,4), (5,5), and (6,6) mechanical modes, respectively. The maximum quantum enhancement is measured for the (6,6) mechanical mode with a 38.4% resolution enhancement and 1.55-fold bandwidth broadening in contrast with a coherent probe. The proposed QEOMA shows significant potential for applications ranging from ultralight dark matter searches to inertial navigation of fast-moving objects. © 2025 Chinese Laser Press

<https://doi.org/10.1364/PRJ.573361>

## 1. INTRODUCTION

Quantum sensing [1–3] harnesses a quantum system or quantum entanglement to estimate a physical quantity, achieving ultrahigh sensitivity or precision beyond the classical limit. The quantum advantage has been demonstrated in numerous photonic platforms including neutral atoms [4], trapped ions [5], Rydberg atoms [6], solid-state spins [7], superconducting circuits [8], and opto-mechanics [9–13]. Nevertheless, the acquired sensitivity is restricted by the imprecision noise stemming from quantum fluctuation of probe laser. The squeezed state [14], whose fluctuation in one quadrature is lower than the shot noise limit, can be tailored to enhance the estimation sensitivity beyond what is achieved classically [15–17]. The squeezing-enhanced technique has been accomplished in multitudinous practical scenarios, such as gravitational wave detection [18–21], magnetometers [22], phase tracking [23,24], biological measurement [25], and force sensing [26].

Acceleration measurement, a flourishing branch of quantum sensing, has become a cornerstone technology for advanced applications, such as gravimeter, inertial navigation [27,28], and dark matter searches [29–32]. To accommodate a wide range of

sensing tasks, the accelerometer must exhibit both high resolution and broad bandwidth. The resolution of traditional microelectromechanical system accelerometers is typically limited to  $\text{mg}/\text{Hz}^{1/2}$  or  $\mu\text{g}/\text{Hz}^{1/2}$  [33,34], and it has been improved by cavity optomechanical accelerometers (COMAs), such as photonic crystal cavities [35], Fabry–Perot fiber microcavities [36,37], membrane-based resonators [31,38,39], and acoustic resonators [32]. By increasing the product of the oscillator mass and quality factor, the resolution of the COMAs can be achieved in the range of  $\text{ng}/\text{Hz}^{1/2}$  to  $\text{pg}/\text{Hz}^{1/2}$  [40]. However, the 3 dB bandwidth is narrowed significantly with the increase of the quality factor. Therefore, there is a trade-off between measurement resolution and bandwidth for arbitrary accelerometers.

Here, we propose and demonstrate a quantum-enhanced optomechanical accelerometer (QEOMA) that integrates an optomechanical accelerometer and quantum squeezed light, simultaneously achieving the improvement of the sensing resolution and bandwidth in contrast with a classical probe. The optomechanical accelerometer is composed of a steerable high reflectivity mirror and an ultralow loss silicon nitride ( $\text{Si}_3\text{N}_4$ ) membrane placed in a vacuum chamber. Thanks to a squeezed

probe, we raise the optomechanical cooperativity and reduce the imprecision noise, driving the bandwidth extension and resolution improvement for the (3,3), (4,4), (5,5), and (6,6) mechanical modes of the  $\text{Si}_3\text{N}_4$  membrane. As a result, we achieve a maximum quantum noise reduction of 4.5 dB, inferring a 38.4% resolution enhancement and 1.55-fold bandwidth broadening in contrast with a coherent probe. The proposed QEOMA holds potential applications in ultralight dark matter detection [29–32], cracks and anomalies in materials [41], and inertial navigation of fast moving objects [42].

## 2. THEORETICAL ANALYSIS

Figure 1(a) illustrates the underlying principle of optomechanical accelerometer. Driven by a probe laser, either coherent or squeezed state of light, the membrane generates a displacement  $x$ , whose equation of motion can be formulated as

$$m \frac{d^2 x(t)}{dt^2} + m\Gamma \frac{dx(t)}{dt} + m\Omega^2 x(t) = F(t), \quad (1)$$

where  $m$  is the effective mass,  $\Gamma$  represents the mechanical damping rate,  $\Omega$  is the resonant angular frequency, and  $F$  denotes the total force acting on the optomechanical accelerometer. After the Fourier transformation  $x(\omega) = \int_{-\infty}^{\infty} x(t) e^{i\omega t} dt$ , the equation of motion can be amended to

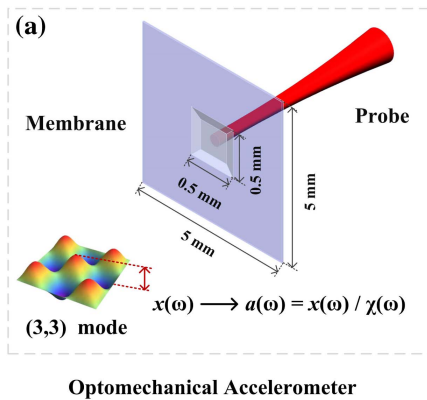
$$-\omega^2 x(\omega) + i\omega\Gamma x(\omega) + \Omega^2 x(\omega) = \frac{F(\omega)}{m} = a(\omega). \quad (2)$$

By solving the foregoing equation, we can obtain  $x(\omega)$ ,

$$x(\omega) = \frac{1}{\Omega^2 - \omega^2 + i\omega\Gamma} a(\omega) = \chi(\omega) a(\omega), \quad (3)$$

where  $\chi(\omega)$  is the mechanical susceptibility. Moreover, the membrane displacement is imprinted on the phase quadrature of probe, thus inferring the membrane acceleration  $a(\omega)$ . The acceleration resolution  $\sqrt{S_a(\omega)}$  can be expressed as

$$\sqrt{S_a(\omega)} = \sqrt{\frac{S_Y(\omega)}{4N C_{\text{eff}} e^{2r} \Gamma |\chi(\omega)|^2} + S_a^{\text{th}}}. \quad (4)$$



The first term represents the imprecision noise, where  $S_Y(\omega)$  is the power spectral density (PSD) in the phase quadrature of probe laser,  $N$  is the average photon number,  $r$  is the squeezing factor, and  $C_{\text{eff}}$  is the effective optomechanical cooperativity of the coherent probe that is approximately constant under the bad-cavity condition. The second term  $S_a^{\text{th}} = \frac{4k_B T \Gamma}{m}$  is the acceleration thermomechanical noise, in which  $k_B$  is Boltzmann's constant and  $T$  represents the temperature. According to Eq. (4), only the mechanical susceptibility  $\chi(\omega)$  is frequency-dependent,  $r$  is dependent of the squeezing strength ( $r = 0$  for a coherent probe), and other parameters can be regarded as constants. According to Eq. (4), off-resonant acceleration resolution is mainly limited by the imprecision noise of the probe beam, while on-resonant resolution is constrained by thermal fluctuations of the accelerometer.

Figure 1(b) displays the theoretical optomechanical acceleration resolution as a function of detuning from resonance frequency. The blue solid curve represents the acceleration resolution with a coherent probe. The minimum resolution at room temperature occurs at the mechanical resonance frequency, as shown by the blue dashed line, while the resolution decreases rapidly away from resonance frequency. Therefore, we can reduce thermal noise and improve resolution performance of the optomechanical accelerometer at resonance frequency by lowering the mechanical damping rate. The red solid curve showcases the acceleration resolution of QEOMA utilizing a  $-10$  dB phase squeezed probe. Apparently, due to the enhanced effective optomechanical cooperativity and reduced mechanical damping rate, the acceleration resolution with a squeezed probe is superior to that with a coherent probe, as indicated by the color-filled region. At off-resonant frequencies, the acceleration resolution is enhanced by 68.3%. The 3 dB bandwidth  $\omega_{(3 \text{ dB})}$  that is proportional to the square root of thermal-to-imprecision-noise ratio [38] has a broadening factor of 2.8 compared with a coherent probe.

## 3. EXPERIMENTAL DIAGRAM

The experimental setup of QEOMA is depicted in Fig. 2. The optical parametric amplifier (OPA) operates in the parametric

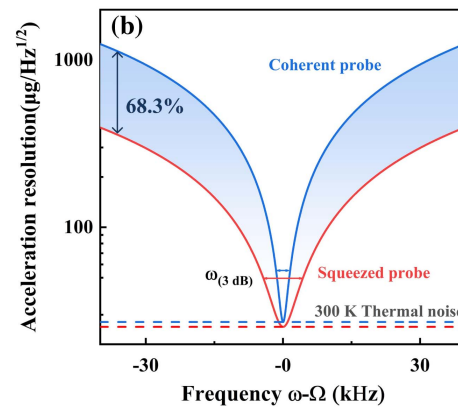


**Fig. 1.** Concept for the optomechanical accelerometer with a higher-order (3,3) mechanical mode (a). Frequency-dependent resolution of the optomechanical accelerometer with different probes (b). The solid blue and red curves represent the acceleration resolution for the coherent probe and the 10 dB squeezed probe, respectively. The dashed blue and red lines show the acceleration thermomechanical noise. The blue shaded region indicates the quantum-enhanced acceleration resolution.

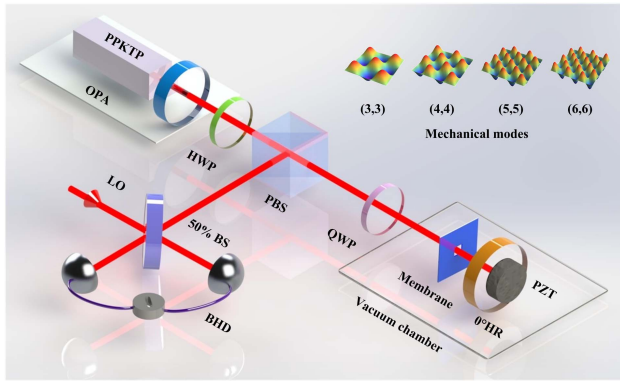


**Fig. 2.** Experimental setup. OPA, optical parametric amplifier; HWP, half-wave plate; PBS, polarizing beam splitter; QWP, quarter-wave plate; 50% BS, 50% beam splitter; BHD, balanced homodyne detector; LO, local oscillator; 0° HR, 0° high reflectivity mirror; PZT, piezoelectric transducer. Inset, the higher-order mechanical modes of the  $\text{Si}_3\text{N}_4$  membrane.

amplification condition and generates a phase-squeezed state [43]. The OPA consists of an output coupler with a curvature radius of 25 mm and a 10-mm-long periodically poled titanyl phosphate crystal with a 12 mm radius of curvature. The pump beam enters the doubly resonant OPA through the output coupler, while the seed beam is introduced from one end of the crystal surface. Both the pump and seed beams resonate within the OPA, and the reflectivity of output coupler is 84.3% at 1550 nm and 97.8% at 775 nm. By stabilizing the OPA length with a pump beam and controlling the relative phase between the pump and seed beams at zero, a bright phase-squeezed state with a quantum noise reduction of  $-7.1 \text{ dB} \pm 0.2 \text{ dB}$  is generated.

The phase-squeezed state that serves as a sensing probe has an output power of  $20 \text{ } \mu\text{W}$ , which is totally transmitted through the polarizing beam splitter (PBS) by adjusting a half-wave plate. After interacting with an optomechanical accelerometer, the reflected probe containing the desired acceleration information is completely reflected by the PBS, and the extraction efficiency is maximized by a quarter-wave plate. The reflected probe then interferes with an 8 mW local oscillator (LO) on a 50% beam splitter and is subsequently detected by a balanced homodyne detector (BHD). During the data acquisition process, the relative phase between the LO and reflected probe is controlled at  $\pi/2$ , measuring the quantum fluctuations of phase quadrature. Finally, the desired acceleration information is extracted from the AC component of BHD and recorded by a spectrum analyzer.

The optomechanical accelerometer is composed of a steerable high reflectivity mirror and a  $\text{Si}_3\text{N}_4$  membrane fabricated by low-pressure chemical vapor deposition. The high-stress (0.9 GPa) membrane on the silicon wafer has a length of 0.5 mm, a thickness of 100 nm, and an effective mass of  $1.7 \times 10^{-11} \text{ kg}$ . It is bonded to three corners of the jarless frame with minimal adhesive droplets. The optomechanical accelerometer is placed in a vacuum chamber at a pressure of  $\mu\text{Torr}$ . To optimize the acceleration response, a ring-shaped piezoelectric transducer is positioned behind the high reflectivity mirror to precisely tune the cavity length.

#### 4. EXPERIMENTAL RESULTS AND DISCUSSION

The normalized PSDs of individual higher-order ( $m, m$ ) mechanical modes for the membrane-based optomechanical accelerometer are illustrated in Fig. 3. The blue and red curves represent the normalized PSDs with a coherent probe and a squeezed probe, respectively. The resonance frequencies are 2.379 MHz for the (3,3) mode, 3.273 MHz for the (4,4) mode, 3.966 MHz for the (5,5) mode, and 4.829 MHz for the (6,6) mode, all aligning with theoretical predictions. Especially for the (6,6) mode, the mechanical damping rate is 14 Hz, yielding a corresponding quality factor  $Q = 3.45 \times 10^5$ . Apparently, thermal noise dominates near the resonance frequency. As the measurement frequency is away from the resonance point, the imprecision noise gradually turns into main limitation. For higher-order mechanical modes, the oscillation amplitude is too small to distinguish from imprecision noise under the condition of the same driving power. Therefore, we do not demonstrate measurement results about higher-order mechanical modes.

Driven by a squeezed probe with identical power, the resonance frequencies of the optomechanical accelerometer are consistent with coherent counterparts. Due to the reduced quantum fluctuations in phase quadrature, the imprecision noise for the (6,6) mechanical mode is reduced by 4.5 dB at frequencies far away from resonance point. In addition, quantum squeezed light increases the equivalent  $Q$  value (from  $3.45 \times 10^5$  to  $4.02 \times 10^5$ ) of the optomechanical accelerometer that corresponds to the reduction of the mechanical damping rate. For the (3,3), (4,4), and (5,5) mechanical modes, the imprecision noise reductions are 1.5 dB, 3.0 dB, and 3.9 dB, respectively, demonstrating the quantum advantage of the QEOMA. The obvious difference of quantum advantage originates from the dependence of the original squeezing factor on the frequency. Here, quantum squeezed light has an original quantum noise reduction of 4.1 dB at 2.379 MHz, 5.6 dB

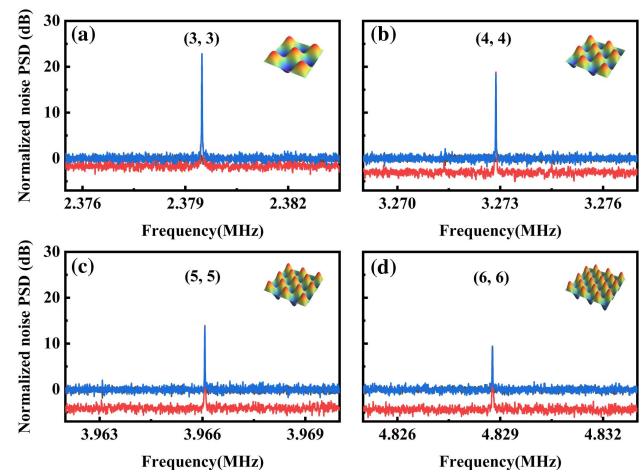


**Fig. 3.** Normalized noise power spectral densities (PSDs) of the optomechanical accelerometer for both coherent and squeezed probes. Panels (a)–(d) correspond to the (3,3), (4,4), (5,5), and (6,6) mechanical modes, respectively. Each experimental curve is averaged over 50 samples with a resolution bandwidth of 10 Hz and video bandwidth of 1 Hz. Inset, the spatial shape for the ( $m, m$ ) mode.

at 3.273 MHz, 6.5 dB at 3.966 MHz, and 7.1 dB at 4.829 MHz, respectively. It can be explained by the frequency-dependent technical noise [44] of the 1550 nm fiber laser. To eliminate the extra technical noise, the mode cleaner with a narrower linewidth can be introduced in both seed and pump beams.

Figures 4(a)–4(d) illustrate the frequency-dependent acceleration resolution for the higher-order (3,3), (4,4), (5,5), and (6,6) modes, which are derived by converting the PSD depicted in Figs. 3(a)–3(d) with Eq. (4). The acceleration resolutions for coherent probes are represented by the blue curves, and the minimum resolution is approximately  $27 \mu\text{g}/\text{Hz}^{1/2}$  occurring at the resonance frequency of the membrane. At the frequency far away from resonance frequency, the acceleration resolutions are reduced to  $150 \mu\text{g}/\text{Hz}^{1/2}$ ,  $210 \mu\text{g}/\text{Hz}^{1/2}$ ,  $250 \mu\text{g}/\text{Hz}^{1/2}$ , and  $310 \mu\text{g}/\text{Hz}^{1/2}$  for the (3,3), (4,4), (5,5), and (6,6) modes, respectively. The difference comes from the frequency-dependent characteristic of the mechanical susceptibility and effective optomechanical cooperativity, which can be easily obtained from Eq. (4).

The acceleration resolutions for the squeezed probe are shown by the red curves. In the off-resonant frequency region, the acceleration resolution for the (6,6) mechanical mode reaches around  $191 \mu\text{g}/\text{Hz}^{1/2}$ , corresponding to a 38.4% resolution improvement compared with the coherent probe. For the (3,3), (4,4), and (5,5) modes, the resolutions improvements at off-resonant frequencies are 16.8%, 27.9%, and 32.7%, respectively. The thermal noise dominates at the resonance frequency, and the resolution improvement is not obvious for any mechanical modes, as shown in the inset of Fig. 4. We conclude, from Fig. 4, that the sensing bandwidth is significantly expanded for all higher-order mechanical modes, demonstrating the quantum advantage of the QEOMA. Especially for the (6,6) mode, the bandwidth is expanded from 2.9 kHz to 4.5 kHz, corresponding to an improvement factor of 1.55.

The minimum acceleration resolution of our membrane-based optomechanical sensor is  $25 \mu\text{g}/\text{Hz}^{1/2}$ , which is inferior to that using a cold atomic interferometer ( $4.6 \text{ ng}/\text{Hz}^{1/2}$ ) [27], monolithic fused silica ( $82 \text{ pg}/\text{Hz}^{1/2}$ ) [40], microchip ( $32 \text{ ng}/\text{Hz}^{1/2}$ ) [37], and  $\text{Si}_3\text{N}_4$  membrane ( $0.6 \mu\text{g}/\text{Hz}^{1/2}$ ) [38]. Generally speaking, the minimum resolution is determined by the intrinsic mechanical properties of the accelerometer, including resonant frequency  $\Omega$ , effective mass  $m$ , mechanical damping rate  $\Gamma$ , and temperature  $T$ . The main limitations of our QEOMA are the  $10^5$  quality factor of commercial  $\text{Si}_3\text{N}_4$  membrane and the 300 K system temperature. In the future, the acceleration resolution will reach the scale of  $\text{ng}/\text{Hz}^{1/2}$  by fabricating the  $\text{Si}_3\text{N}_4$  membrane with a higher quality factor ( $10^9$ ) [31], cooling the  $\text{Si}_3\text{N}_4$  membrane to 100 mK [35,39], and reducing the mechanical damping rate [45–47]. Moreover, the off-resonant resolution can be further improved by designing a high-finesse “membrane-in-middle” resonator [48] to increase the optomechanical cooperativity.

The acquired quantum advantage is immensely dependent of the initial squeezing parameter and channel efficiency. In order to optimize the squeezing parameter, one can eliminate the extra technical noise of fiber laser, increase the escape efficiency of OPA, and improve the phase stability between pump and seed beams [49–55]. The channel efficiency can be increased by improving the interference efficiency between local oscillator and signal beam, improving the quantum efficiencies of photodiodes, and utilizing ultralow-loss optical components including the  $\text{Si}_3\text{N}_4$  membrane, polarization beam splitter, wave plates, and lens.

## 5. CONCLUSION

In summary, we have presented a quantum-enhanced optomechanical accelerometer (QEOMA) with a maximum resolution improvement of 38.4% and bandwidth broadening of 1.55-fold in contrast with a coherent probe. By leveraging a quantum squeezed light, the multi-parameters of the

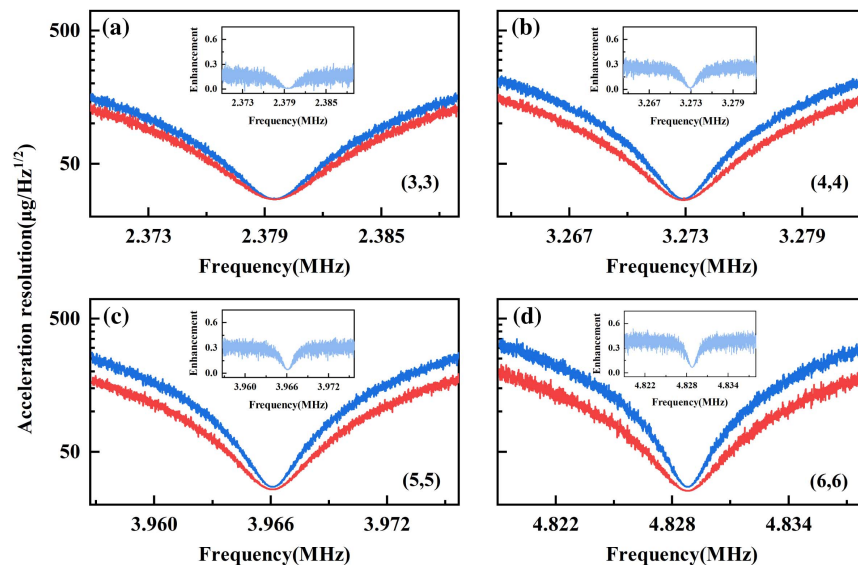


**Fig. 4.** Acceleration resolution of the membrane-based optomechanical accelerometer for different probes. The resonance frequencies are consistent with those shown in Fig. 3. Inset, acceleration resolution advantage with a squeezed probe at different frequencies.

optomechanical accelerometer, including the optomechanical cooperativity, the imprecision noise, and the mechanical damping rate, were significantly improved, simultaneously achieving the improvement of the sensing resolution and bandwidth. Independent of the resonance frequency for the mechanical modes, we, respectively, demonstrated the quantum advantage of the optomechanical accelerometer for the (3,3), (4,4), (5,5), and (6,6) modes, corresponding to the resonance frequency of 2.379 MHz, 3.273 MHz, 3.966 MHz, and 4.829 MHz. The proposed QEOMA can be conveniently expanded to other cavity optomechanical accelerometers and applied to numerous domains including ultralight dark matter searches and inertial navigation of fast-moving objects.

**Funding.** National Natural Science Foundation of China (62225504, 12274275, 62027821, U22A6003, 62375162, 12304399, 12174234); Key R&D Program of Shanxi (202302150101004).

**Disclosures.** The authors declare no conflicts of interest.

**Data Availability.** Data underlying the results presented in this paper are not publicly available at this time but may be obtained from the authors upon reasonable request.

## REFERENCES

- C. L. Degen, F. Reinhard, and P. Cappellaro, "Quantum sensing," *Rev. Mod. Phys.* **89**, 035002 (2017).
- B. J. Lawrie, P. D. Lett, A. M. Marino, *et al.*, "Quantum sensing with squeezed light," *ACS Photonics* **6**, 1307–1318 (2019).
- A. A. Clerk, M. H. Devoret, S. M. Girvin, *et al.*, "Introduction to quantum noise, measurement, and amplification," *Rev. Mod. Phys.* **82**, 1155–1208 (2010).
- I. Baumgart, J. M. Cai, A. Retzker, *et al.*, "Ultrasensitive magnetometer using a single atom," *Phys. Rev. Lett.* **116**, 240801 (2016).
- M. Brownnutt, M. Kumph, P. Rabl, *et al.*, "Ion-trap measurements of electric-field noise near surfaces," *Rev. Mod. Phys.* **87**, 1419–1482 (2015).
- S. Gleyzes, S. Kuhr, C. Guerlin, *et al.*, "Quantum jumps of light recording the birth and death of a photon in a cavity," *Nature* **446**, 297–300 (2007).
- S. Aigner, L. D. Pietra, Y. Japha, *et al.*, "Long-range order in electronic transport through disordered metal films," *Science* **319**, 1226–1229 (2008).
- D. Halbertal, J. Cuppens, M. B. Shalom, *et al.*, "Nanoscale thermal imaging of dissipation in quantum systems," *Nature* **539**, 407–410 (2016).
- S. Barzanjeh, A. Xuereb, S. Gröblacher, *et al.*, "Optomechanics for quantum technologies," *Nat. Phys.* **18**, 15–24 (2022).
- B. B. Li, L. F. Ou, Y. C. Lei, *et al.*, "Cavity optomechanical sensing," *Nanophotonics* **10**, 2799–2832 (2021).
- M. Aspelmeyer, T. J. Kippenberg, and F. Marquardt, "Cavity optomechanics," *Rev. Mod. Phys.* **86**, 1391–1452 (2014).
- Z. Shen, Z. Zhou, C. Zou, *et al.*, "Observation of high-Q optomechanical modes in the mounted silica microspheres," *Photonics Res.* **3**, 243–247 (2015).
- B. B. Li, G. Brawley, H. Greenall, *et al.*, "Ultrabroadband and sensitive cavity optomechanical magnetometry," *Photonics Res.* **8**, 1064–1071 (2020).
- C. Xu, L. Zhang, S. Huang, *et al.*, "Sensing and tracking enhanced by quantum squeezing," *Photonics Res.* **7**, A14–A26 (2019).
- W. Yao, X. Zhang, L. Tian, *et al.*, "Loss-tolerant and supersensitive angular rotation estimation based on quantum-enhanced interferometers," *Phys. Rev. A* **110**, 032429 (2024).
- K. Zheng, M. Mi, B. Wang, *et al.*, "Quantum-enhanced stochastic phase estimation with the SU(1,1) interferometer," *Photonics Res.* **8**, 1653–1661 (2020).
- J. Liu, W. Liu, S. Li, *et al.*, "Enhancement of the angular rotation measurement sensitivity based on SU(2) and SU(1,1) interferometers," *Photonics Res.* **5**, 617–622 (2017).
- W. Jia, V. Xu, K. Kuns, *et al.*, "Squeezing the quantum noise of a gravitational-wave detector below the standard quantum limit," *Science* **385**, 1318–1321 (2024).
- J. Lough, E. Schreiber, F. Bergamin, *et al.*, "First demonstration of 6 dB quantum noise reduction in a kilometer scale gravitational wave observatory," *Phys. Rev. Lett.* **126**, 041102 (2021).
- M. J. Yap, J. Cripe, G. L. Mansell, *et al.*, "Broadband reduction of quantum radiation pressure noise via squeezed light injection," *Nat. Photonics* **14**, 19–23 (2020).
- L. Kleybolte, P. Gewecke, A. Sawadsky, *et al.*, "Squeezed-light interferometry on a cryogenically cooled micromechanical membrane," *Phys. Rev. Lett.* **125**, 213601 (2020).
- B. B. Li, J. Bilek, U. B. Hoff, *et al.*, "Quantum enhanced optomechanical magnetometry," *Optica* **5**, 850–856 (2018).
- H. Yonezawa, D. Nakane, T. A. Wheatley, *et al.*, "Quantum-enhanced optical-phase tracking," *Science* **337**, 1514–1517 (2012).
- J. Yu, Y. Qin, J. Qin, *et al.*, "Quantum enhanced optical phase estimation with a squeezed thermal state," *Phys. Rev. Appl.* **13**, 024037 (2020).
- M. A. Taylor, J. Janousek, V. Daria, *et al.*, "Biological measurement beyond the quantum limit," *Nat. Photonics* **7**, 229–233 (2013).
- Y. Xia, A. R. Agrawal, C. M. Pluchar, *et al.*, "Entanglement-enhanced optomechanical sensing," *Nat. Photonics* **17**, 470–477 (2023).
- Z. Yu, B. Fang, L. Chen, *et al.*, "Memory-assisted quantum accelerometer with multi-bandwidth," *Photonics Res.* **10**, 1022–1030 (2022).
- Y. Huang, J. G. FlorFlores, Y. Li, *et al.*, "A chip-scale oscillation-mode optomechanical inertial sensor near the thermodynamical limits," *Laser Photonics Rev.* **14**, 1800329 (2020).
- D. Carney, G. Krnjaic, D. C. Moore, *et al.*, "Mechanical quantum sensing in the search for dark matter," *Quantum Sci. Technol.* **6**, 024002 (2021).
- A. J. Brady, X. Chen, Y. Xia, *et al.*, "Entanglement-enhanced optomechanical sensor array with application to dark matter searches," *Commun. Phys.* **6**, 237 (2023).
- J. Manley, M. D. Chowdhury, D. Grin, *et al.*, "Searching for vector dark matter with an optomechanical accelerometer," *Phys. Rev. Lett.* **126**, 061301 (2021).
- J. Manley, D. J. Wilson, R. Stump, *et al.*, "Searching for scalar dark matter with compact mechanical resonators," *Phys. Rev. Lett.* **124**, 151301 (2020).
- M. Metcalfe, "Applications of cavity optomechanics," *Appl. Phys. Rev.* **1**, 031105 (2014).
- J. Lin, L. Pham, R. Tao, *et al.*, "A 4 kHz, 25  $\mu\text{g}/\sqrt{\text{Hz}}$ , 3-axis MEMS accelerometer ASIC using beyond-resonant-frequency sensing," in *IEEE Custom Integrated Circuits Conference (CICC)* (2023), pp. 1–2.
- A. G. Krause, M. Winger, T. D. Blasius, *et al.*, "A high-resolution microchip optomechanical accelerometer," *Nat. Photonics* **6**, 768–772 (2012).
- F. G. Cervantes, L. Kumanchik, J. Pratt, *et al.*, "High sensitivity optomechanical reference accelerometer over 10 kHz," *Appl. Phys. Lett.* **104**, 221111 (2014).
- F. Zhou, Y. Bao, R. Madugani, *et al.*, "Broadband thermomechanically limited sensing with an optomechanical accelerometer," *Optica* **8**, 350–356 (2021).
- M. D. Chowdhury, A. R. Agrawal, and D. J. Wilson, "Membrane-based optomechanical accelerometry," *Phys. Rev. Appl.* **19**, 024011 (2023).
- W. Li, W. Liu, C. Liu, *et al.*, "Broadband optomechanical accelerometer reaching the thermomechanical limit based on suspended membrane resonator," *IEEE Sens. J.* **24**, 17528–17536 (2024).
- A. Hines, A. Nelson, Y. Zhang, *et al.*, "Compact optomechanical accelerometers for use in gravitational wave detectors," *Appl. Phys. Lett.* **122**, 094101 (2023).

41. Z. Qin, T. Zhu, L. Chen, *et al.*, "High sensitivity distributed vibration sensor based on polarization-maintaining configurations of phase-OTDR," *IEEE Photonics Tech. L.* **23**, 1091–1093 (2011).
42. S. Liu, J. Hu, B. Li, *et al.*, "Chip-scale integrated optical gyroscope based on a multi-mode co-detection technique," *Photonics Res.* **13**, 319–329 (2025).
43. X. Sun, W. Li, Y. Tian, *et al.*, "Quantum positioning and ranging via a distributed sensor network," *Photonics Res.* **10**, 2886–2892 (2022).
44. X. Sun, Y. Wang, L. Tian, *et al.*, "Dependence of the squeezing and anti-squeezing factors of bright squeezed light on the seed beam power and pump beam noise," *Opt. Lett.* **44**, 1789–1792 (2019).
45. G. Huang, A. Beccari, N. J. Engelsen, *et al.*, "Room-temperature quantum optomechanics using an ultralow noise cavity," *Nature* **626**, 512–516 (2024).
46. A. H. S. Naeini, J. T. Hill, S. Meenehan, *et al.*, "Two-dimensional phononic-photon band gap optomechanical crystal cavity," *Phys. Rev. Lett.* **112**, 153603 (2014).
47. G. S. Maccabe, H. Ren, J. Luo, *et al.*, "Nano-acoustic resonator with ultralong phonon lifetime," *Science* **370**, 840–843 (2020).
48. D. Mason, J. Chen, M. Rossi, *et al.*, "Continuous force and displacement measurement below the standard quantum limit," *Nat. Phys.* **15**, 745–749 (2019).
49. Y. Tian, Y. Wang, W. Wang, *et al.*, "Reservoir-engineered squeezed lasing through the parametric coupling," *Phys. Rev. Lett.* **134**, 243803 (2025).
50. S. Shi, L. Tian, Y. Wang, *et al.*, "Demonstration of channel multiplexing quantum communication exploiting entangled sideband modes," *Phys. Rev. Lett.* **125**, 070502 (2020).
51. L. Gao, L. Zheng, B. Lu, *et al.*, "Generation of squeezed vacuum state in the millihertz frequency band," *Light Sci. Appl.* **13**, 294 (2024).
52. Y. Sun, Y. Tian, Y. Wang, *et al.*, "Squeezing level strengthened by a temperature dependent dispersion compensation methodology," *Opt. Commun.* **530**, 129192 (2023).
53. W. Li, M. Ju, Q. Li, *et al.*, "Squeezing-enhanced resolution of radio-frequency signals," *Chin. Opt. Lett.* **22**, 072701 (2024).
54. Y. Wu, Q. Wang, L. Tian, *et al.*, "Multi-channel multiplexing quantum teleportation based on the entangled sideband modes," *Photonics Res.* **10**, 1909–1914 (2022).
55. X. Sun, Y. Wang, Y. Tian, *et al.*, "Deterministic and universal quantum squeezing gate with a teleportation-like protocol," *Laser Photonics Rev.* **16**, 2100329 (2022).